Rare Metal Materials and Engineering
Volume 48, Issue 4, April 2019
Available online at www.rmme.ac.cn

Science Press

Cite this article as: Rare Metal Materials and Engineering, 2019, 48(4): 1079-1086.

ARTICLE

Influence of δ Phase on the Microstructure and Properties of Inconel 625 Superalloy Tubes

Gao Yubi, Ding Yutian, Meng Bin, Ma Yuanjun, Chen Jianjun, Xu Jiayu

State Key Laboratory of Advanced Processing and Recycling of Nonferrous Metals, Lanzhou University of Technology, Lanzhou 730050, China

Abstract: The amount, distribution and morphology of δ phase in Inconel 625 superalloy were controlled by cold deformation and aging treatment. The characteristic of δ phase was characterized by X-ray diffraction (XRD), scanning electron microscopy (SEM) and energy dispersive spectrometer (EDS). The influence of δ phase on the microstructure and properties of Inconel 625 superalloy tubes was investigated. The results show that the average grain size decreases, the deformation uniformity of the grain becomes better gradually, and the hardness increases, with the increase of cold deformation (ε). The δ phase firstly precipitates at the deformation twin and grain boundaries as well as deformation bands, and then precipitates within the grains. The precipitation of needle δ phase is oriented in two near-orthogonal directions or a lattice-like distribution within the grain, while oriented in two parallel directions at the deformation bands. With the increase of cold deformation, the morphology of δ phase varies gradually from needle to spheroid or short rodlike. The average grain size of the alloy decreases with the increase of cold deformation and the extension of aging time (t). The hardness of the alloy increases with the extension of aging time when the cold deformation is 35%, but there is no obvious change in the hardness of the alloy with the extension of aging time as the cold deformation is more than 50%.

Key words: Inconel 625 superalloy; δ phase precipitation; pinning effect; solute drag; microstructure and property

Nickel based wrought superalloy Inconel 625 is a solid solution strengthening superalloy with face centered cubic (fcc) structure, which is mostly strengthened by the additions of molybdenum (Mo) and niobium (Nb)[1,2]. The alloy has been widely used in aerospace, marine, chemical, petrochemical, and nuclear industries, due to its high tensile, creep and rupture strength, outstanding fatigue and thermal fatigue strength, oxidation resistance, excellent weldability, processsability, and resistance to high temperature corrosion on prolonged exposure to aggression[3-5]. Although the alloy was initially designed as a solid solution strengthened nickel-base superalloy, it has been shown subsequently that the precipitation of intermetallic phases occurs in the alloy during aging treatments or during service[6]. Unlike the majority of precipitation hardening nickel-base superalloys in which strengthening is brought about mainly by precipitates of γ'-Ni_3(Al, Ti) phase having ordered face-centered cubic $L1_2$ structure, in Inconel 625 alloy, precipitation hardening is caused primarily by precipitates of γ''-Ni_3(Nb, Mo) phase, which has the ordered body-centered tetragonal DO_{22} structure and is coherent with the γ matrix[7,8]. This phase provides very high strength at low-to-intermediate temperatures (550~650 °C), but it is unstable at temperatures above about 650 °C[9]. The metastable γ'' phase transforms to the equilibrium intermetallic δ phase of Ni_3(Nb, Mo) composition. The δ-Ni_3(Nb, Mo) phase, orthorhombic DO_a structure, is invariably incoherent with the γ matrix. This phase can form directly from the supersaturated γ matrix when aging temperatures is higher than 750 °C[3,10]. The metastable γ'' phase gets transformed to the equilibrium δ phase after aging for a long time in the temperature range from 650 °C to 750 °C[11].

For Inconel 625 superalloy tubes in medium and high temperature (600~900 °C) environment during long-term aging or service, the metastable phase γ'' easily transformed

Received date: April 20, 2018
Foundation item: National Natural Science Foundation of China (51661019)
Corresponding author: Ding Yutian, Ph. D., Professor, State Key Laboratory of Advanced Processing and Recycling of Nonferrous Metals, Department of Materials Science and Engineering, Lanzhou University of Technology, Lanzhou 730050, P. R. China, E-mail: dingyutian@126.com

into the equilibrium δ phase, or δ phase directly formed in the γ matrix precipitation, which resulted in that the alloy performance was deteriorated, the alloy tubes premature failure occurred, and then the service life of the alloy tubes was greatly shortened[12,13]. Therefore, in the aging or service process of Inconel 625 superalloy tubes, the controlling of δ phase plays a critical role in the development of optimal mechanical properties, which depends strongly on the amount, distribution and morphology of δ phase.

In recent years, numerous researchers and technologists have worked to study the δ phase nucleation mechanism, precipitation kinetics, precipitation temperature, precipitation law and coarsening of Inconel 625 superalloy[11,14-16]. However, the effect of the δ phase on mechanical properties has seldom been examined in detail. The work reported here is undertaken as a part of a detailed study aiming at the characterization of the δ phase that develops in Inconel 625 superalloy after prolonged service or aging at 800 °C under different cold deformation. The aim of this work is to investigate the crucial role of cold deformation control in the amount, distribution and morphology of the precipitation of δ phase, as well as δ phase's influence on the microstructure and properties to ensure optimal performance of the alloy in the aging or service.

1 Experiment

The chemical composition (mass fraction, %) of Inconel 625 superalloy used in this investigation is as follows: 0.042 C, 21.77 Cr, 0.19 Co, 8.79 Mo, 0.21 Al, 0.40 Ti, 3.68 Fe, 3.75 Nb, 0.12 Si, 0.2 Mn, 0.0006 S, 0.006 P, 0.06 Cu and balance Ni. The material was manufactured by vacuum induction melting (VIM) and electro-slag remelting (ESR) process. The ingot was hot extruded into a tube with Φ159 mm × 18 mm. Cylindrical specimens of 6 mm in diameter and 9 mm in height were machined from hot extrusion tubes of Inconel 625 superalloy. The specimens were solution treated at 1150 °C for 1 h and then quenched into air cooling, before room temperature compression test. The deformation degree ε of room temperature compression test was 35%, 50% and 65% at the strain rate of 10^{-1} s^{-1}. After room temperature compression testing, the specimens were aged at 800 °C for 25, 50, 75 and 100 h followed by cooling in air. Then, the deformed and aged specimens were sliced along the compression axis for microstructure characterization.

The sliced specimens were ground, mechanically polished and then chemically etched in a solution consisting of 3 mL HNO_3+5 mL H_2SO_4+90 mL HCl at room temperature for 1~3 min for metallographic observation, which were conducted using a Axiovert 40 MAT optical microscope (OM). The average grain size of the specimens was obtained according to standard test methods for characterizing duplex grain sizes (GB/T 24177-2009), the maximum grain size D_{max} and the highest probability of distribution grain size D_K were obtained, and the non-uniform factor $Z=D_{max}/D_K$ was used to assess microstructure uniformity[17,18]. The morphology and distribution of δ phase were observed using a Quanta FEG 450 thermal field emission scanning electron microscopy (SEM) and energy dispersive spectrometer (EDS). The hardness value of the alloy was measured using an FRC-3e Rockwell hardness tester and the hardness value was the average of three groups.

The crystal structure and the lattice parameters of the δ phase were tested using a D8 ADVANCE type X-ray diffraction (XRD) with Cu radiation at 40 kV and 40 mA. All specimens were scanned in the standard geometry from 20° to 100° with 0.02° step size and 1 s dwelling time. The position of diffraction peaks was corrected with Si power. The integrated intensities of the diffraction peaks of δ and γ phases were calculated using a software package. The lattice constants of γ phase were calculated with the Nelson-Riley extrapolation method.

Fig.1 is the time-temperature-transformation diagram of the phase in Inconel 625 superalloy[2,19], which indicates only the δ phase precipitates in the γ matrix at aging temperature of 800 °C for 25 h to 100 h. The mass fraction of δ phase can be determined by the direct comparison method[20]. In this method, the mass fraction of δ phase can be determined by the following equation:

$$W_\delta = \frac{1}{1+\frac{\rho_\gamma}{\rho_\delta}\cdot\frac{\frac{1}{n}\sum_i^n (I_i^\gamma / R_i^\gamma)}{\frac{1}{m}\sum_i^m (I_i^\delta / R_i^\delta)}} \quad (1)$$

where, W_δ is the mass fraction of δ phase, I_i^δ and I_i^γ are the integrated intensities of the (201), (020), (012) and (211) peaks of δ phase, and the (111), (200), (220), (311) and (222) peaks of γ phase, respectively. ρ_δ and ρ_γ are the volume density of the δ and γ phase, respectively, and n and m are the number of selected diffraction lines. R_i is the intensity factor and can be expressed as

$$R_i = \frac{1}{v^2} P_i F_i \varphi(\theta) e^{-2M} \quad (2)$$

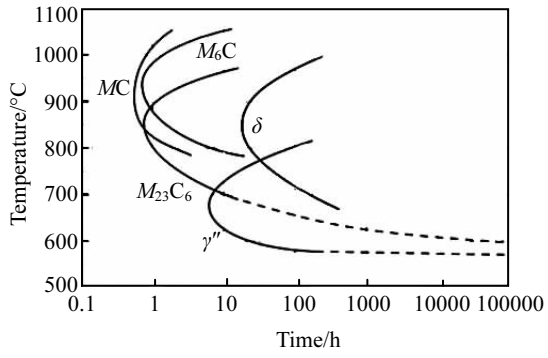

Fig.1 Time-temperature-transformation diagram of the phase in Inconel 625 superalloy[2,19]

where, v is the precise volume of unit cell, P_i is the multiplicity factor of the diffraction plane, F_i is the structure factor, $\varphi(\theta)$ is the Lorentz and Polarization factor, and e^{-2M} is the temperature factor. The structure factor F_i associated with δ phase has been given by Sundararaman et al[11], and the value of F_i is calculated according to the composition of δ phase[21]. The calculated values according to Eq. (2) were given in Ref. [22].

2 Results and Discussion

2.1 Microstructure and properties of alloy after cold deformation

Fig.2 shows the optical micrographs of Inconel 625 superalloy tubes under different cold reductions. The microstructure exhibits equiaxed grains with average grain size about 31.03 μm (Fig.2a). Under the 35% cold deformation, the microstructure is composed of equiaxed grains and a few deformation twins, and the grains are slightly elongated (Fig.2b). Since the Inconel 625 superalloy is a low stacking fault energy material, this low stacking fault energy can not only reduce the cross-slip ability of dislocation during cold deformation process of the specimen, but also decrease the interface energy of twin boundaries, causing that the stress of alloy reaches the desired stress of the deformation twins before dislocation movement. Thus, deformation twins in cold deformation process occur readily in lower stacking fault energy alloys[23]. For the 50% cold deformation, the grains show obviously compressive deformation and exhibit flattened shape, as well as a large number of deformation twins and deformation bands appear in the microstructure (Fig.2c). With cold deformation increasing to 65%, the degree of grain deformation is larger, and the grains exhibit thin-strip in shape. Meanwhile, the deformation bands and slip lines increase, as well as the grain boundaries and the loading pressure axis are arranged vertically (Fig.2d). This is because that the slip surface of the Inconel 625 superalloy, with crystal rotating due to the reaction shaft rupture, the crystal in the slip at the same time, ultimately turns to the direction perpendicular to the force in the process of compression deformation, as shown in Fig.3. For the polycrystalline material, due to constraints of the grain boundaries and other microstructure factors, each grain in the slip process also requires rotation. This leads to the change of the force axis orientation correspond to the crystal, showing that the grain boundaries and the loading pressures axis are arranged vertically[24].

Fig.4 shows the microstructure uniformity and grain size of Inconel 625 superalloy tubes under different cold reductions. It can be seen that the average grain size decreases and the non-uniform factor Z declines with the increase of cold deformation, which indicates that the deformation uniformity of the grains are better gradually. For one thing, it is because that the Inconel 625 superalloy has a face-centered cubic structure and the γ matrix is austenitic. Besides, the close-packed plane with the largest atomic density is {111} crystal plane at which the slip the crystal mostly preferentially occurs. For another thing, when the strain accumulation is large enough, the multiple slip system launches and cross-slip occurs, so that the dislocations are crossed to form a cell-like substructure. However, the crystal orientation is mainly {111} plane, which indicates that the grain boundaries are directional rotation along the pressure axis in the process of compression

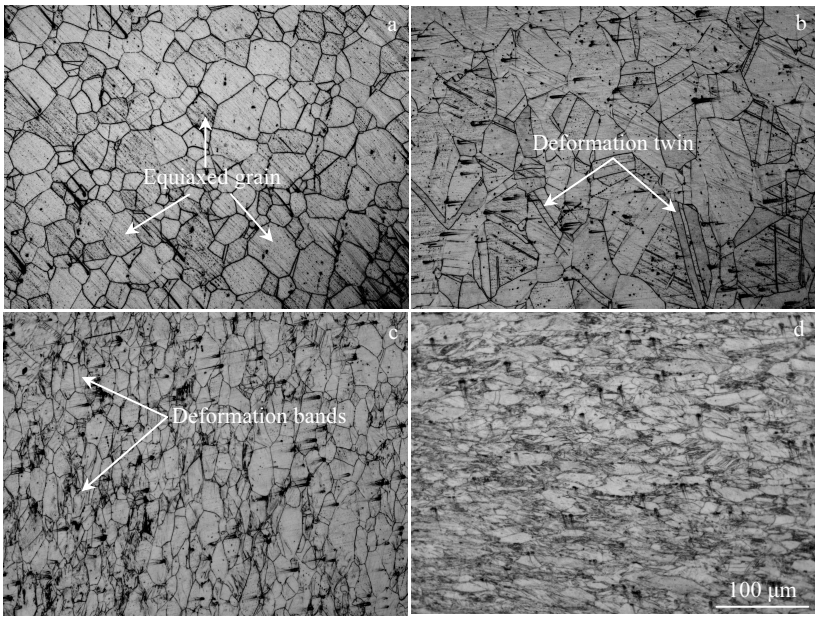

Fig.2 Microstructures of Inconel 625 superalloy tube under different cold reductions: (a) ε=0%, (b) ε=35%, (c) ε=50%, and (d) ε=65%

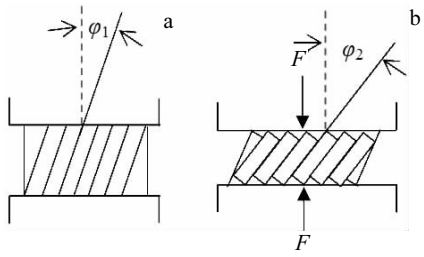

Fig.3 Rotation of crystal in crystal compression ($\varphi_2>\varphi_1$): (a) before compression and (b) after compression

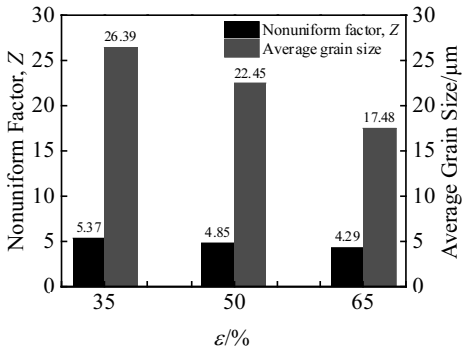

Fig.4 Effects of cold reduction on the microstructure uniformity and grain size of Inconel 625 superalloy tubes

deformation after the grain beginning to break, so that the grain orientation distribution tends to be consistent with it after refinement[25], as shown in Fig.5.

The variation law of the hardness of Inconel 625 superalloy tubes under different cold reductions is shown in Fig.6. It can be observed that the hardness of the alloy increases with the increase of cold reduction. The compression deformation process in Inconel 625 superalloy changes not only grain shapes, but also the crystal structure including the formation of vacancies and deformation twins, lattice distortion as well

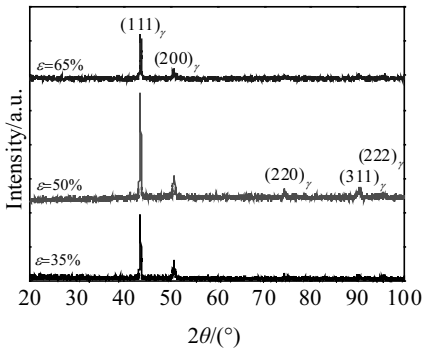

Fig.5 XRD patterns of Inconel 625 superalloy tubes under different cold reductions

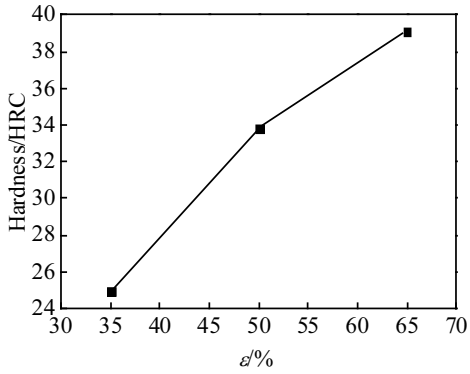

Fig.6 Effect of cold reduction on hardness of Inconel 625 superalloy tubes

as the increase of dislocation density and so on. Thus, these changes will be directly expressed in the alloy macroscopic mechanical properties, such as the increase of deformation resistance and hardness, while the decrease of toughness, causes an obvious working hardening phenomenon[26].

2.2 XRD qualitative and quantitative analysis

Fig.7 represents the XRD patterns of Inconel 625 superalloy tubes under different cold reductions and aging time. Lattice parameters of the δ phase were determined on the basis of XRD results obtained from specimens containing significant mass fraction of this phase. The values obtained from specimens of the same alloy subjected to different aging treatments show small variations. As determined by XRD qualitative and quantitative analysis, lattice parameters of γ and δ phase in Inconel 625 are a=0.3572 nm, a=0.5106 nm, respectively, with b=0.4251 nm and c=0.4556 nm. These values are quite similar to those reported by Sundararaman et al[11]. For Inconel 625, the mass fraction of δ phase determined by XRD techniques is given in Fig.8. It has been found that the mass fraction of δ phase increases with the increase of cold reduction and the extension of the holding time. In Inconel 625 superalloy, heterogeneous nucleation of δ phase occurs at both intergranular and intragranular, whose nucleation sites are related to the temperature. At the aging temperature of 800 °C for 25 h to 100 h, only the δ phase precipitates in the γ matrix. Cold deformation creates a large number of crystal defects, such as vacancies, dislocations and grain boundaries. With the increase of cold deformation, the number of vacancies and dislocations increases. On the one hand, the defects provide favorable nucleation sites of δ phase. On the other hand, this defects storing energy can reduce the nucleation energy to promote the δ phase nuclei. As a result, cold deformation promotes precipitation of δ phase.

2.3 Morphologies and distribution of the δ phase

The SEM images of δ phase under different cold deformation in Inconel 625 superalloy is shown in Fig.9. It is interesting to note that cold deformation alters not only the

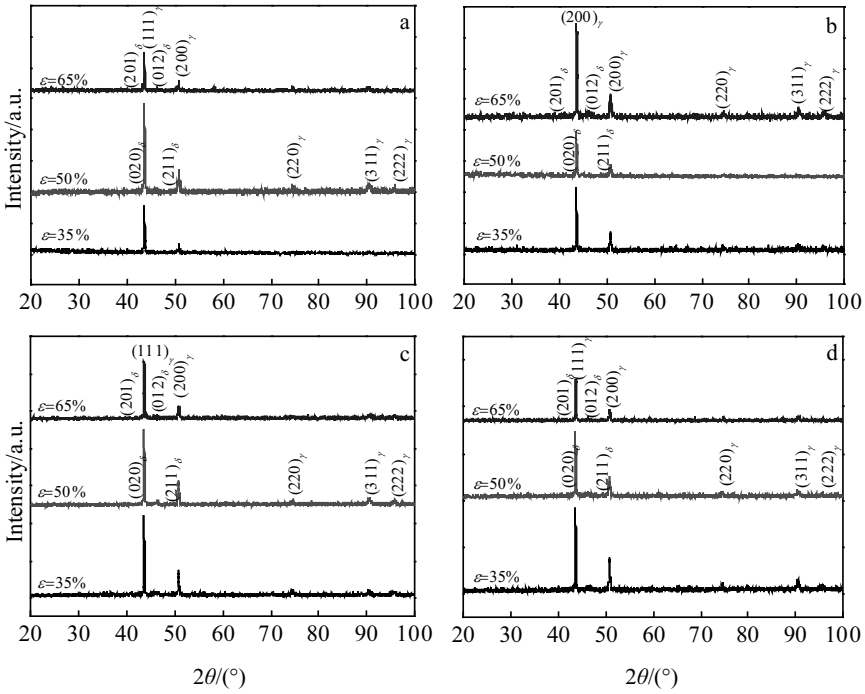

Fig.7 XRD patterns of Inconel 625 superalloy tubes under different cold reductions and aging time: (a) t=25 h, (b) t=50 h, (c) t=75 h, and (d) t=100 h

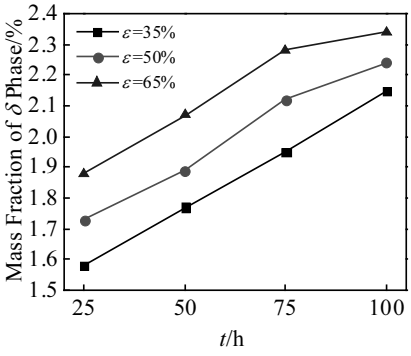

Fig.8 Precipitation law of δ phase in Inconel 625 superalloy tubes under different cold reductions and aging time

precipitation morphology but also the precipitation sites of δ phase. The precipitation of needle δ phase is oriented in two near-orthogonal directions or a lattice-like distribution within the grain, while oriented in two parallel directions at the deformation bands. For the 35% cold deformation specimen, the δ phase firstly precipitates at the deformation twin and grain boundaries, and subsequently precipitates in the grains, which exhibits the needle morphology (Fig.9a). For the above 50% cold deformation specimen, the δ phase first precipitates at the deformation twin and grain boundaries as well as deformation bands (Fig.9b), and then precipitates in the grains (Fig.9c). The amount of δ phase at deformation bands increases and the morphology of δ phase varies gradually from needle to short rodlike or spheroid with the increase of cold deformation. It is because that short rodlike or spheroid morphology of δ phase can be attracted to Nb atoms segregating vacancy to absorb defects, such as dislocation cell walls, twin and grain boundaries, through the mechanism of nonequilibrium segregation. Since the local Nb super-saturation as the nucleation catalysts is increased, it can be expected that cold deformation affects the thermodynamics of δ phase[27]. Therefore, δ phase can grow into γ matrix and connect to each other to form needle morphology with a small cold deformation. Thus, the amounts of Nb atom segregation at dislocation cell walls, twin and grain boundaries where δ phase nucleation sites are limited, while only δ phase can grow in the morphology of short rodlike or spheroid around twin and grain boundaries or dislocation cell walls with the increase of cold deformation[28]. As a result, the morphology of δ phase varies gradually from needle to spheroid or short rodlike with cold deformation increasing.

The EDS scan along the line of δ phase of Inconel 625 superalloy is shown in Fig.10. It can be seen that the degree of Nb segregation in the γ matrix is less than that at the twin and grain boundaries (Fig.10a) as well as deformation bands (Fig.10b), so that the Nb atoms are enriched in twins and grain boundaries as well as deformation bands due to the effect of Nb nonequilibrium segregation. These results are quite close

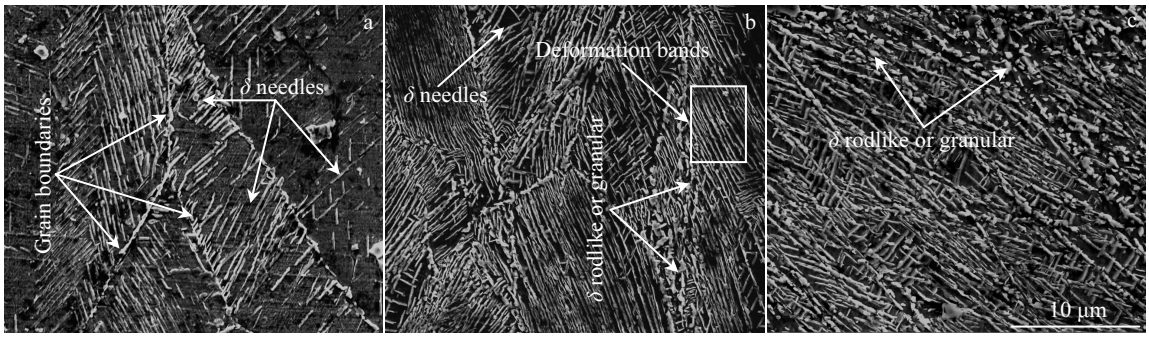

Fig.9 SEM images of δ phase in Inconel 625 superalloy tubes under different cold deformation (t=50 h): (a) ε=35%, (b) ε=50%, and (c) ε=65%

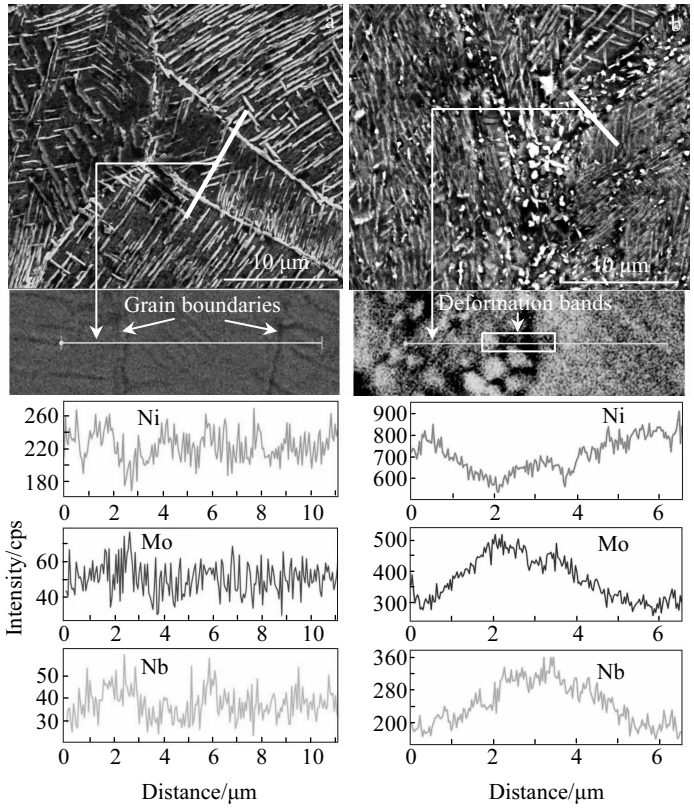

Fig.10 EDS scan along the line of δ phase of Inconel 625 superalloy: (a) ε=35%, t=75 h; (b) ε=50%, t=75 h

to those reported in Ref. [29]. As a result, it indirectly reflects the precipitation of δ phase caused by the Nb nonequilibrium segregation.

2.4 Influence of δ phase on grain size and hardness

Fig.11 shows the microstructures of Inconel 625 tubes under different cold reductions at aging temperature 800 °C for 500 h. It can be seen that the δ phase precipitates at the grain and twin boundaries, which has a pinning effect on the grain and twin boundaries and plays a role in preventing the migration of grain boundaries. Therefore, the average grain size of Inconel 625 superalloy tubes decreases with the increase of cold reduction and the extension of the aging time, which indirectly shows that the grain size decreases with the increase of the amount of δ phase (Fig.12). It is because that the nonequilibrium segregation degree of Nb atoms increases with the increase of cold deformation and the extension of the aging time, and Nb atoms are enriched at dislocation cell walls and twin and grain boundaries, so that the diffusion rate of the Nb solute atoms is much lower than that of the matrix atoms, and the Nb solute atoms at the grain boundaries will hinder the migration of grain boundaries[30]. As the same time, the amount of δ phase precipitating at the twin and grain boundaries increases with the increase of cold deformation and the extension of the aging time, and δ phase plays a pinning role and prevents the migration of grain boundaries[31]. As a result, the solute drag of Nb in solid solution and pinning

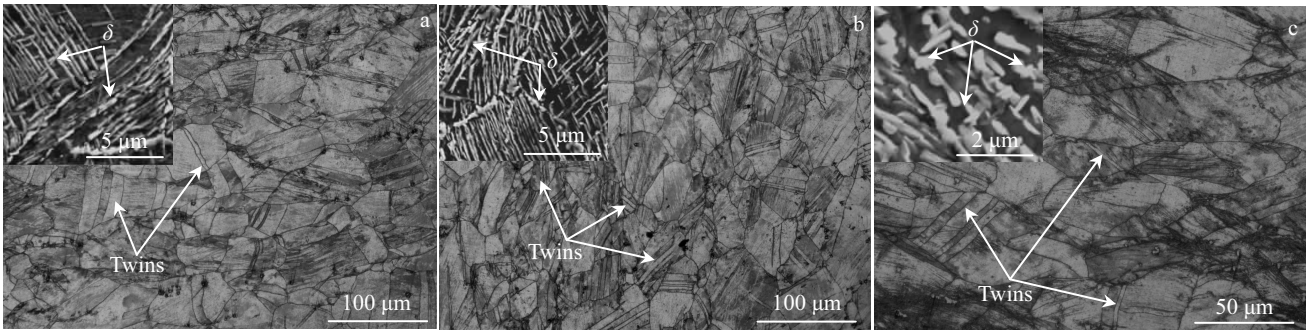

Fig.11 Microstructures of Inconel 625 superalloy tubes under different cold reductions (t=50 h): (a) ε=35%, (b) ε=50%, and (c) ε=65%

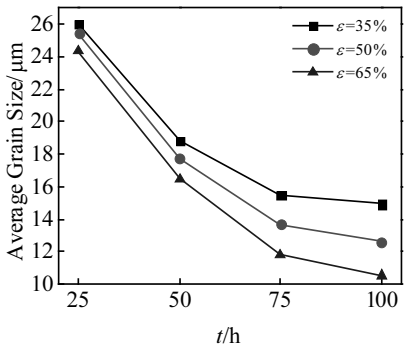

Fig.12 Effect of aging time on grain size of Inconel 625 superalloy tubes

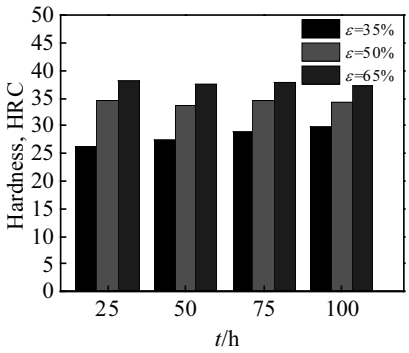

Fig.13 Effect of aging time on hardness of Inconel 625 superalloy tubes

of δ phase inhibits the migration of grain boundaries in the crystal structure, resulting in a significant inhibition of grain growth during aging or service.

The change law of the hardness of Inconel 625 superalloy tubes under different aging time and cold reductions is shown in Fig.13. For the 35% cold deformation specimens, the hardness of the alloy increases with the extension of the aging time. When the deformation is more than 50%, the hardness of the alloy shows no obvious change with the extension of the aging time. For a small cold deformation, needle δ phase precipitates at the twin and grain boundaries, which plays a pinning role and improves the strength of the alloy. For a large cold deformation, needle δ phase can vary to short rodlike or spheroid morphology and the presence of δ phase both in twin and grain boundaries and within the grains can control the grain growth. Moreover, δ phase spheroid morphology is uniformly distributed in the γ matrix, which results in that the dislocation can not be cut, but can only bypass the way through δ phase, thus increasing the obstruction of the dislocation. The increase of the external force causes the dislocation to be obstructed to bend, the adjacent bending lines are connected together, and the dislocation passes through the δ phase and then leaves the small dislocation loops, which plays a role of dispersion strengthening, thereby increasing the strength of the alloy. Besides, the amount of δ phase increases with the increase of cold deformation and the extension of aging time. Meanwhile, the precipitation of δ phase depletes a lot of Nb and Mo atoms playing a solid solution strengthening role in the γ matrix, and the decrease in the amount of Nb and Mo reduces the alloy strength of the alloy (Fig.10). As a result, the hardness of the alloy increases with the extension of aging time when cold deformation is 35%, but there is no obvious change in the hardness of the alloy as the cold deformation is more than 50%.

3 Conclusions

1) The cold deformation behavior of the studied superalloy is strongly sensitive to the strain. With the increase of cold deformation, the average grain size decreases, the deformation uniformity of the grain becomes better gradually, as well as the hardness increases.

2) The δ phase precipitation behavior of the studied superalloy depends on the cold deformation. Cold deformation promotes precipitation of δ phase. The δ phase firstly precipitates at the deformation twin and grain boundaries as well as deformation bands, and then precipitates within the

grains. The precipitation of needle δ phase is oriented in two near-orthogonal directions within the grain while oriented in two parallel directions at the deformation bands. At the same time, the morphology of δ phase varies gradually from needle to spheroid or short rodlike with cold deformation increasing.

3) The average grain size of the alloy decreases with the increase of cold deformation and the extension of aging time. The hardness of the alloy increases with the extension of aging time when cold deformation is 35%, but there is no obvious change in the hardness of the alloy with the extension of aging time as the cold deformation is more than 50%.

References

1 Pollock T M, Tin S. *J Propul Power*[J], 2006, 22(2): 361
2 Shoemaker L E. *Superalloys*[C]. Warrendale, PA: TMS, 2005: 409
3 Shankar V, Rao K B S, Mannan S L. *J Nucl Mater*[J], 2001, 288: 222
4 Ahmad M, Akhter J I, Shahzad M *et al*. *J Alloy Compd*[J], 2008, 457(1-2): 131
5 Thomas C, Tait P. *Int J Pres Ves Pip*[J], 1994, 59(1-3): 41
6 Eiselstein H L, Tillack D J. *Superalloys*[C]. Warrendale, PA: TMS, 1991: 1
7 Sundararaman M, Kumar L, Prasad G E *et al. Metall Mater Trans A*[J], 1999, 30(1): 41
8 Tarzimoghadam Z, Rohwerder M, Merzlikin S V *et al. Acta Mater*[J], 2016, 109: 69
9 Belan J. *Mater Today Proceedings*[J], 2016, 3(4): 936
10 Kirman I, Warrington D H. *Metall Trans A*[J], 1970, 1: 2667
11 Sundararaman M, Mukhopadhyay P, Banerjee S. *Metall Trans A*[J], 1988, 19(3): 453
12 Cortial F, Corrieu J M, Vernot-Loier C. *Metall Mater Trans A*[J], 1995, 26(5): 1273
13 Suave L M, Cormier J, Villechaise P *et al*. *Metall Mater Trans A*[J], 2014, 45: 2963
14 Di X J, Xing X X, Wang B S. *Acta Metall Sin*[J], 2014, 50(3): 323 (in Chinese)
15 Ding Y T, Gao Y B, Dou Z Y *et al*. *Acta Metall Sin*[J], 2017, 53(6): 695 (in Chinese)
16 Liu D X, Zhang X, Qin X Q *et al. Mater Sci Technol*[J], 2017, 33(14): 1610
17 Ma M Y, Chang T J, Gu Z G. *Phys Exam Text*[J], 1990(1): 5 (in Chinese)
18 Yang L, Dong J X, He Z Y *et al. Journal of University of Science and Technology Beijing*[J], 2012, 32(4): 410 (in Chinese)
19 Floreen S, Fuchs G E, Yang W J. *Superalloys*[C]. Warrendale, PA: TMS, 1994: 13
20 Liu W C, Xiao F R, Yao M *et al*. *Scripta Mater*[J], 1997, 37(1): 53
21 Liu W C, Yao M, Chen Z L. *Metall Mater Trans A*[J], 1999, 30(1): 31
22 Liu W C, Xiao F R, Yao M *et al*. *J Mater Sci Letters*[J], 1997, 16(9): 769
23 Peng C H, Chang H, Hu R *et al. J Aeronaut Mater*[J], 2011, 31(2): 8 (in Chinese)
24 Song W X. *Metallic*[M]. Beijing: Metallurgical Industry Press, 2014: 142 (in Chinese)
25 Guo T B, Ding Y T, Yuan X F *et al*. *Chin J Nonferrous Met*[J], 2011, 21(2): 384 (in Chinese)
26 Huang C X, Yang G, Gao Y L *et al. Mater Sci Eng A*[J], 2008, 485(1-2): 643
27 Liu W C, Chen Z L, Xiao F R *et al. Acta Aeronaut Astronaut Sin*[J], 1999, 20(3): 279 (in Chinese)
28 Liu W C, Yao M, Xiao F R *et al. Iron and Steel*[J], 1997, 32(5): 55 (in Chinese)
29 Liu W C, Yao M, Chen Z L *et al. J Mater Sci*[J], 1999, 34(11): 2583
30 Cahn J W. *Acta Metall Sin*[J], 1962, 10: 907 (in Chinese)
31 Smith C S. *Trans Met Soc AIME*[J], 1948, 175: 15

δ 相对 Inconel 625 合金管材组织及性能的影响

高钰璧，丁雨田，孟　斌，马元俊，陈建军，许佳玉

(兰州理工大学 省部共建有色金属先进加工与再利用国家重点实验室，甘肃 兰州 730050)

摘　要：通过冷变形及时效处理来调控 Inconel 625 合金中 δ 相的含量、分布及形貌，采用 XRD、SEM 和 EDS 表征 δ 相的特征，研究了 δ 相对 Inconel 625 合金管材组织及性能的影响。研究表明，随着冷变形量的增加，合金的平均晶粒尺寸减小，晶粒变形均匀性逐渐变好，合金的硬度增加；δ 相首先在形变孪晶界、晶界及变形带上析出，随后在晶内析出，针状的 δ 相在晶内呈近正交状或网格状分布，而在变形带上平行排列；随着冷变形量的增加，δ 相的形貌由针状转变为短棒状或颗粒状；合金的平均晶粒尺寸随着冷变形量的增加和保温时间的延长而减小；当冷变形量为 35%时，合金的硬度随保温时间的延长而增加，而冷变形量超过 50%时合金的硬度没有发生明显的变化。

关键词：Inconel 625 合金；δ 相；钉扎作用；溶质拖曳；组织性能

作者简介：高钰璧，男，1991 年生，博士生，兰州理工大学材料科学与工程学院，甘肃 兰州 730050，E-mail: gaoyubi1991@126.com